5-26-2015

The Arched Flexure VSA: A Compact Variable Stiffness Actuator with Large Stiffness Range

Joseph M. Schimmels
Marquette University, joseph.schimmels@marquette.edu

Daniel Garces
Marquette University

The Arched Flexure VSA: A Compact Variable Stiffness Actuator with Large Stiffness Range

Joseph M. Schimmels
Department of Mechanical Engineering, Marquette University, Milwaukee, WI
Daniel R. Garces
Milwaukee Electric Tool, Milwaukee, WI

Abstract:

The high stiffness of conventional robots is beneficial in attaining highly accurate positioning in free space. High stiffness, however, limits a robot's ability to perform constrained manipulation. Because of the high stiffness, geometric conflict between the robot and task constraints during constrained manipulation can lead to excessive forces and task failure. Variable stiffness actuators can be used to adjust the stiffness of robot joints to allow high stiffness in unconstrained directions and low stiffness in constrained directions. Two important design criteria for variable stiffness actuation are a large range of stiffness and a compact size. A new design, the Arched Flexure VSA, uses a cantilevered beam flexure of variable cross-section and a controllable load location. It allows the joint to have continuously variable stiffness within a finite stiffness range, have zero stiffness for a

small range of joint motion, and allow rapid adjustment of stiffness. Using finite element analysis, flexure geometry was optimized to achieve high stiffness in a compact size. A proof-of-concept prototype demonstrated continuously variable stiffness with a ratio of high stiffness to low stiffness of 55.

SECTION I. Introduction

Conventional robots use high stiffness joints and position control to provide very good absolute positioning accuracy in free space. Conventional robots, however, are not good at performing constrained manipulation tasks that may involve geometric conflict. Because of the robot high stiffness, geometric conflict would cause very large contact forces. A conventional robot, then, would either penetrate the constraint or be stopped by the constraint, potentially damaging the robot and/or the constraining object and likely causing manipulation task failure.

When performing constrained manipulation, some form of compliance is needed to accommodate discrepancies between the task model and the actual locations of tasks constraints. Robot compliance is also needed to attain the “soft robot” behavior identified as safe and effective for human-robot collaboration [1].

One means of obtaining more compliant robots is to add compliance at the robot joints. Robots with series elastic actuators [2] have shown to be beneficial in manipulation tasks. Joints with serial elastic actuators have a relatively stiff spring between the actuator and the next link. Variable stiffness actuators are similar, but use a spring with controllable stiffness [3], [1], [4], [5] between the motor and the link. As summarized in [5], the use of variable stiffness actuation is motivated by: 1) improved safety to human coworkers and to itself, 2) greater efficiency in energy storage and more rapid release in walking and impact, and 3) much better robustness to errors in the model of the robot or its environment.

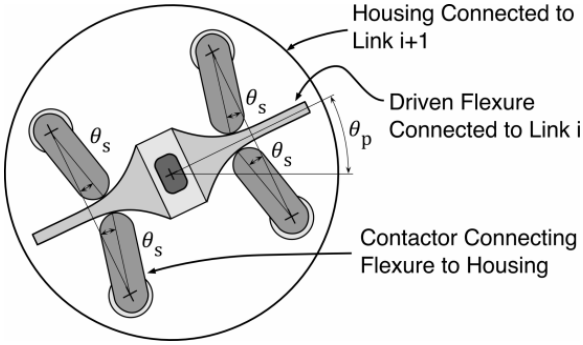

Fig. 1. The arched flexure VSA schematic representation. The changing contact points with the flexure provides the stiffness changes.

In a review of *variable stiffness actuation* (VSA) approaches [3], four distinct strategies were identified. They are: 1) equilibrium controlled stiffness, 2) antagonistic controlled stiffness, 3) mechanically controlled stiffness, and 4) structure controlled stiffness. An equilibrium controlled VSA uses a spring in series with an actuator and changes the equilibrium point of the spring. An antagonistic controlled VSA uses two similar sized actuators connected to one shaft via nonlinear elastic elements. A mechanically controlled VSA adjusts the effective stiffness of the system, always using the full spring length. A structure controlled VSA adjusts the effective stiffness of the system by changing the physical structure of the spring.

Here, a new type of structure controlled variable stiffness actuator [6] is presented. The new design, illustrated in Figure 1, consists of a conventional drive motor and two additional components that constitute a variable stiffness spring. These components are: 1) an arched cantilevered beam flexure, and 2) a contactor (4 are illustrated in Fig. 1). The flexure is rigidly connected to the drive motor shaft. The 4 contactors are each connected to a housing by a revolute joint. The housing is rigidly connected to the link to be moved. The flexure

and contactor together provide the actuator variable stiffness that is controlled by an additional small motor. The stiffness is varied by changing the location of where the contactor meets the flexure along its length. When the contact point is close to the motor shaft, the effective flexure stiffness is high; when the contact point is further away, the flexure effective stiffness is low. In this arched flexure design, the flexure beam effective length, its thickness, its width, and the direction of constraining forces all cause an increase in the beam effective stiffness as the contactor moves closer to the motor shaft.

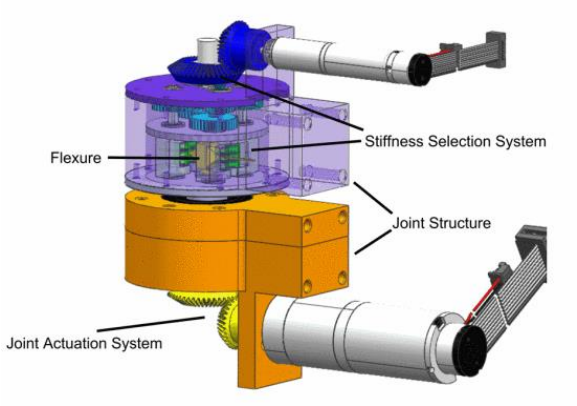

Fig. 2. CAD model of the arched flexure VSA

This paper describes the design, the design methodology, and the performance of the Arched Flexure VSA. Section II identifies the key functions of the VSA. Section III provides an overview of the analysis used to evaluate flexure stiffness and optimize flexure geometry. Section IV summarizes the performance of the VSA that was fabricated and tested. Section V provides a brief discussion and summary of the work.

SECTION II. Arched Flexure VSA Components

As stated previously, the Arched Flexure VSA design concept is capable of large change in stiffness despite being small in size. The overall VSA design includes the design of 3 key subsystems illustrated in Figure 2. They are: 1) the stiffness selection system, 2) the joint drive system, and 3) the overall joint structure. The stiffness selection system provides the connection between the flexure and the next link. It changes the stiffness value by changing the contact point on the flexure and transfers forces from the flexure to the next link. The joint drive system moves the flexure and generates the torque needed to drive the connected link. The overall joint structure provides mounting locations for all components, including the adjacent links. It also provides the structural integrity of the VSA so that it restricts motion in all other directions other than the 1 degree of freedom about the joint axis.

A. Stiffness Selection System

As shown in Fig. 1, the flexure beam effective length, area moment of inertia, and force application angle all change as the the contactor bar rotates (θ_s changes). The contactor bar provides the connection between the flexure and the next link through the joint housing. The joint stiffness can be changed rapidly with a small change in contactor angle θ_s. The design and optimization of the flexure geometry is described in detail in Section III.

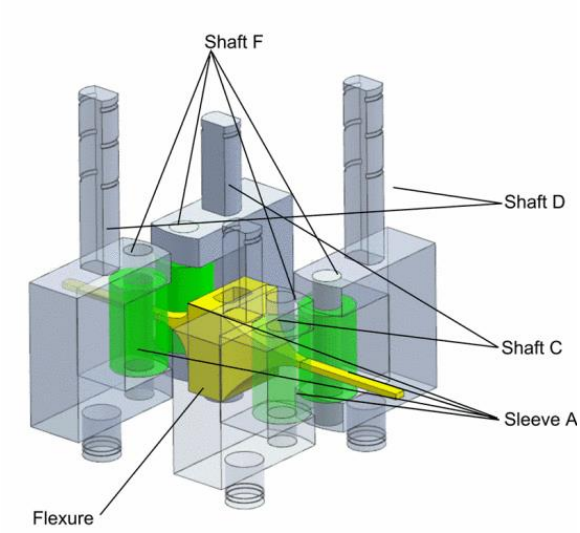

Fig. 3. CAD model of the contactor subsystem

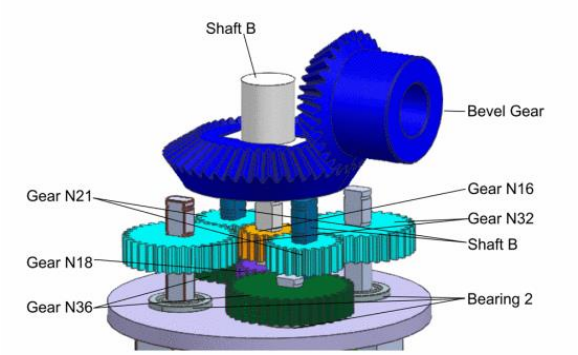

Fig. 4. CAD model of stiffness selection system gearing

Note that, in addition to the large continuous change in stiffness with contactor angle, the Arched Flexure VSA will also allow the joint to have zero stiffness for a limited range of joint motion when $\theta_s < 0$. The extended length flexure (which includes the section in which the cross sectional area is constant) allows the contactor bars to recapture the flexure after contact is lost during free joint motion.

The contactor system shown in Fig. 3 consist of 4 shafts (2 each of Shafts C and D), each with a C-shaped contact bar that supports bearings that roll along the flexure to allow low friction motion along the flexure.

Because the structure controlled Arched Flexure VSA does not require constant power to maintain a specific stiffness value and because the contactor motion is only along the flexure, the contactor system is driven by a single low-power actuator (a Maxxon DCXI0L with gear ratio of 64:1). This actuator drives the bevel gear (near the top of Fig. 4) with gear ratio of 1.5:1. The bevel gear is attached to a central shaft that drives the contactor subsystem. The gear train (illustrated in Fig. 4) drives 2 contactor shafts (Shaft C) in one direction and 2 shafts (Shaft D) in the opposite direction to adjust joint stiffness each with a gear ratio of 2:1. The gear ratio for the complete system driving each of the 4 contactors is 192:1.

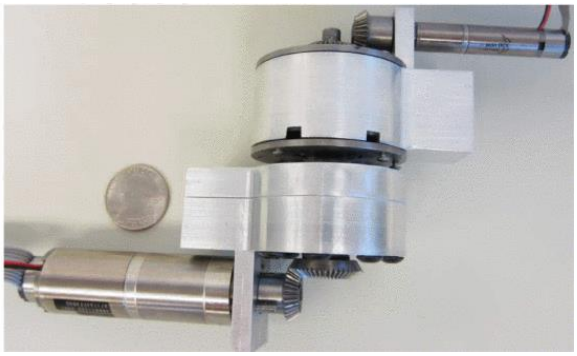

Fig. 5. Arched flexure VSA prototype

B. Joint Actuation System

The joint is driven by a single actuator (Maxxon DCX22S) that is connected to a bevel gear that together with the integrated gear head provides a gear ratio of 364.5:1. The bevel gear is connected to the joint shaft which is rigidly connected to the arched flexure. Actuator position directly determines flexure position θ_p and ultimately the position of the connected robot link.

C. Overall Joint Structure

The joint structure protects the stiffness selection system, ensures that the VSA maintains kinematic integrity (1 DOF only) despite load, and provides connections to the adjacent links. The connections of links and motors to the joint structure are located on different planes orthogonal to the joint axis to prevent interference so that the VSA provides a full 360 degrees of rotation.

The fully assembled Arched Flexure VSA prototype is pictured in Figure 5. Note that the stiffness selection system (flexure and gear train) are contained within the joint structure.

SECTION III. Flexure Geometry Optimization

An important component of the stiffness selection system is the arched flexure. Its force-deflection characteristics largely determine the range of stiffness that can be achieved by the VSA. The curvature of the arch largely determines the size of the VSA. The analysis and optimization of the flexure are described below in terms of the geometric parameters of the arched flexure. The geometric parameters illustrated in Fig. 6 are:

	x-position of center of arch curvature
R_1	flexure arch curvature in plane of contactor bars
R_2	center hole radius
R_3	flexure arch curvature out of contactor bar plane
θ_1	maximum angle of the curved portion of flexure
θ_2	maximum angle of load application
H_f	flexure distal height
W_f	flexure distal width

Each of the length parameters was normalized (relative to R_2), to obtain a set of 7 dimensionless parameters that fully define the flexure shape and that are easily scaled for different sized actuators. (The x-location for the center of curvature for R_3 was selected to be the same as that for R_1.)

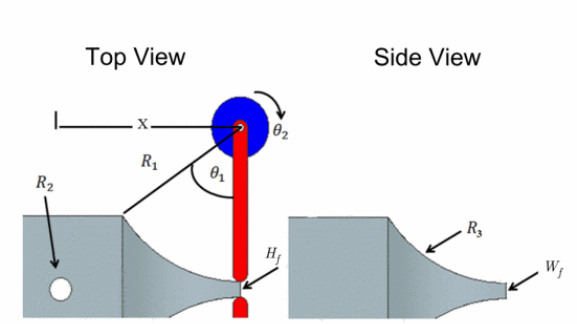

Fig. 6. Parameters used to describe flexure geometry

Due to the significant change in the beam thickness along its length, standard beam theory cannot be used to determine the flexure force-deflection characteristics. Instead, *finite element analysis* (FEA) was used to determine flexure stiffness for different loading locations. FEA takes complex shapes and breaks those shapes into a large number of cubes and tetrahedrons that, when connected together (the mesh), closely approximate the complex shape being analyzed. The mesh was constructed to allow loading along the *line of contact* between the flexure and contactor for a variety of loading locations. The FEA program used for the analysis, ANSYS, has its own programming language with a text file input which lends itself for use in optimization.

A. Optimization Strategy

The flexure optimization was performed by combining the finite element analysis of ANSYS with the optimization routines of MatLab. Using a set of values for the parameters identified above, the MatLab program generates a text file containing the ANSYS code describing the flexure shape and loading conditions. ANSYS performs the analysis and generates an output text file containing the flexure original and deformed geometry for each of the different load application locations. MatLab reads this text file to determine the effective stiffness of the flexure for each loading condition and evaluates performance of the design. To optimize the flexure, the geometry is modified and this sequence is repeated until a “best flexure” is identified.

The joint effective stiffness, k, is calculated using the FEA node displacement information. The displacement of those nodes where the force was applied are used to calculate angular displacement δ_θ using

$$\delta_\theta = \arctan\left(\frac{\delta_y}{l - \delta_l}\right)$$

(1)

where δ_y is the change in position in the transverse direction of the nodes at the location that the force is applied, δ_l is the change in position in the axial direction of the nodes at the location that the force is applied, and l is the distance from the axis of rotation to the load location.

The effective stiffness is calculated using

$$k = \frac{T}{\delta_\theta}$$

(2)

where T is the applied torque.

The stiffness of the flexure is calculated for a variety of load locations along the flexure. This stiffness evaluation is used to assess the quality of the different flexure geometries in the optimization procedure.

Important aspects of an optimization are the objective function and the design constraints. These are described below.

1) Objective Function

Important criteria in the evaluation of flexure geometry include the range in stiffness values that can be achieved for the different load locations and the ability to accurately select the desired stiffness. The best flexure is one that minimizes the objective function $f(x)$ given by

$$f(x) = \log\left(\frac{k_{min}}{k_{max}}\right) + WD$$

(3)

where k_{min} is the lowest stiffness of the flexure which occurs when the load is applied at the flexure distal location, k_{max} is the maximum joint stiffness which occurs when the load is applied near the drive shaft, D is the least squares fit error to an exponential function (associated with relative sensitivity), and W is the weighting factor used to indicate the relative importance of the 2 criteria.

The relative sensitivity term D indicates how closely the stiffness variation with contactor angle θ_s approximates an exponential function. An exponential stiffness variation with contactor angle would ensure constant relative sensitivity of the stiffness to uncertainty in contactor angle positioning. This would ensure that stiffness sensitivity to contactor angle is low when the stiffness is low and sensitivity is high when stiffness is high and would change smoothly throughout its range. This is expressed mathematically by

$$\frac{dk/d\theta_s}{k} = \mathrm{c}$$

where c is the rate of exponential growth.

The stiffness ratio component of the objective function considers the range of stiffness without regard to how smoothly the stiffness increases with contactor angle. A good flexure design will maximize the ratio $\frac{k_{max}}{k_{min}}$ or equivalently minimize its reciprocal. By convention, the objective function is minimized.

2) Constraint Functions

Optimization constraint functions are used to restrict the set of possible solutions. These constraints address physically imposed limits as well as some imposed for consistency with ANSYS input requirements. The lowercase variables are dimensionless equivalents of the uppercase length variables (normalized by R_2) that were defined previously. By convention, optimization constraints are expressed is the form: $g(x \leq 0$. The constraints expressed in this form are:

$$
\begin{aligned}
g_1(x) &= r_1 \cos\theta_1 - r_1 - \frac{h_f}{2} - x + 1.5 \le 0 \\
g_2(x) &= r_3 \cos\theta_1 - r_3 - \frac{w_f}{2} + 1.5 \le 0 \\
g_3(x) &= r_1 \sin\theta_1 - x + 1.5 \le 0 \\
g_4(x) &= r_3 \sin\theta_1 - x + 1.5 \le 0 \\
g_5(x) &= \theta_2 - \theta_1 + \frac{\pi}{18} \le 0 \\
g_6(x) &= r_1 - x + 0.6667 \le 0 \\
g_7(x) &= r_3 - x + 0.6667 \le 0 \\
g_8(x) &= \theta_2 - \tan\left(\frac{x}{h_f/2 + r_1}\right) + 0.05 \le 0
\end{aligned}
$$

(4)(5)(6)(7)(8)(9)(10)(11)

View Source

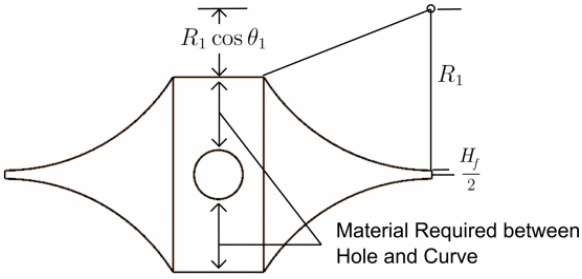

Fig. 7. Geometry associated with constraint g_1

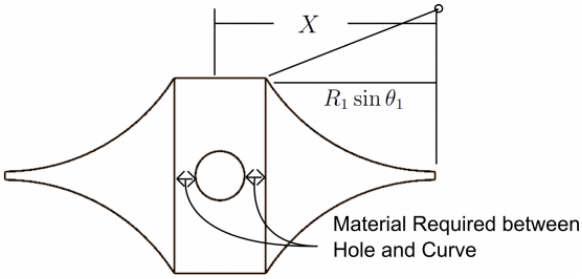

Fig. 8. Geometry associated with constraint g_3

Constraints g_1 and g_2 require that the flexure has sufficient material to ensure its structural integrity near the shaft mounting hole, specifically that the remaining material has a thickness of at least half of the hole radius. Figure 7 illustrates the constraint g_1 geometry in the plane of the contactor bars.

Similarly, constraints g_3 and g_4 ensure that the shaft mounting hole is not larger than the flat area of the flexure. This constraint is needed to maintain consistency with the mesh generated for the ANSYS model. Figure 8 illustrates constraint g_3 geometry for the plane of the contactor bars.

Constraint g_5 ensures that the load is not applied too close to the end of the arch. If the load is applied near the edge, the lack of sufficient material would allow the contactor bar to slide off of the arched portion of the flexure.

Constraints g_6 and g_7 ensure that the flexure will maintain the same set of flexure features regardless of specified geometric values, specifically the flat portions near the shaft mounting hole. Without these constraints, ANSYS will attempt to generate a mesh that is inconsistent with the geometry specified.

Table I Optimal flexure geometry

Dimensionless Parameters	Optimal Value	
	$W = 0$	$W = .025$
x	8.733	7.735
r_1	8.000	7.240
r_3	8.143	6.625
h_f	0.333	1.033
w_f	0.361	0.531
θ_1	1.007	0.961
θ_2	0.776	0.783

Constraint g_8 ensures that the line of action of the load will impart a moment on the shaft in the same direction throughout the range of load locations.

B. Optimization Procedure

The genetic algorithm in the Matlab global optimization toolbox was used to find the flexure geometry that minimized the objective function of Eq. 3 subject to the constraints of Eqs. 4–11.

To increase the speed of the optimization, two different FEA models were used in different stages of the optimization. The FEA model used in the first stage of the optimization had a relatively coarse grid. It was used to refine the search area while using less computing time. The geometry obtained from the first stage of the optimization was use as input as the starting locations for the second stage of the optimization using a more refined mesh in the FEA model. This second phase optimization used the highest level of grid refinement allowed when using ANSYS in batch mode.

An evaluation of the force-deflection characteristics of a single flexure geometry using the coarse grid FEA model takes about three minutes in ANSYS; whereas an evaluation using the fine grid FEA model takes about 7 minutes. The time required to perform a complete optimization was about 8 days on a conventional PC.

C. Flexure Optimization Results

Results were obtained for the optimal flexure for 2 different weighting factor values (values of W in Eq. 3). In one case, the constant relative sensitivity was deemed to be unimportant ($W = \mathbf{0}$); and in the other, the 2 criteria were deemed to be about equally important ($W = \mathbf{0.25}$; selected based on multiple trials). The optimal flexure dimensionless geometry for each of the 2 cases is summarized in Table I.

Figure 9 illustrates the variation of joint stiffness k with contactor selection angle θ_s for the maximum stiffness range optimization ($W = \mathbf{0}$). The results for three levels of grid refinement are shown to illustrate that a higher level of grid refinement does not significantly influence results. With a higher level of grid refinement, the high stiffness values are reduced, but the low stiffness values remain approximately the same. The 14k node model was used as the coarse grid evaluation in the stage 1 optimization. The 30k node model was used as the fine grid evaluation in the stage 2 optimization. It is the highest resolution that can be used when ANSYS is run in batch mode. Higher grid resolutions can be used when ANSYS is run in interactive mode.

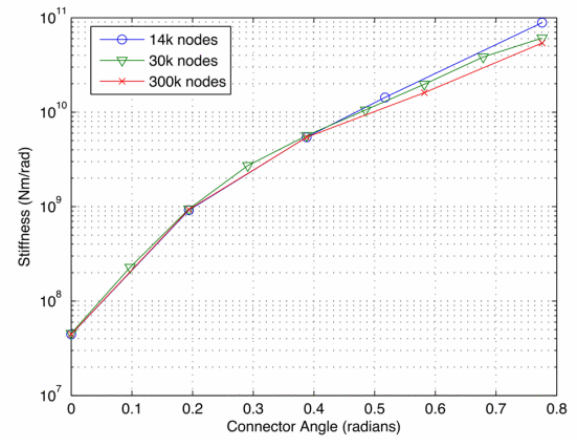

Fig. 9. Optimal stiffness vs. Contactor angle for $W = \mathbf{0}$

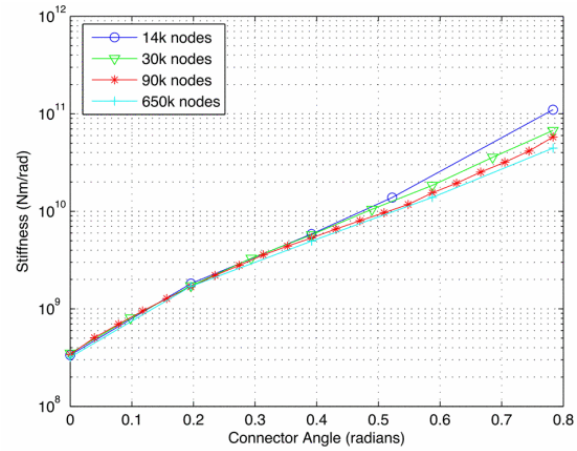

Fig. 10. Optimal stiffness vs. Contactor angle for $W = \mathbf{0.25}$

Figure 10 illustrates the variation of joint stiffness k with contactor selection angle θ_s for the optimization in which stiffness range and relative sensitivity are deemed to be approximately equal in importance ($W = \mathbf{0.25}$). Similar to the previous results, Fig. 10 shows that the lower stiffness values all match at the four levels of mesh refinement, while the higher stiffness values do not match as well. The calculated stiffness values decrease as the mesh refinement level increases.

SECTION IV. Experimental Performance

An arched flexure VSA prototype optimized for both stiffness range and relative sensitivity ($W = \mathbf{0.25}$) was fabricated and is illustrated in Fig. 5. To obtain high yield strength with low plastic deformation, the flexure was made of titanium. Experiments were conducted to determine whether the design met targeted performance.

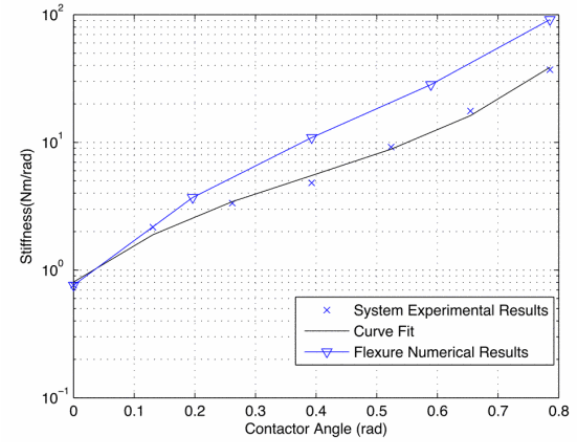

Fig. 11. Experimental results for stiffness vs. Contactor angle

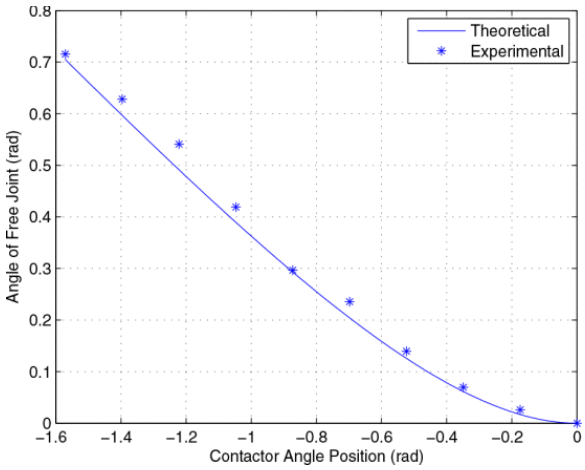

Fig. 12. Contactor angular position vs free joint range for free joint angles

The results of an experiment to determine the relationship between joint stiffness k and contactor angle θ_s are provided in Fig. 11. The theoretical results for the flexure alone obtained using ANSYS are also provided for comparison. Theoretical and experimental values are very similar at low values of stiffness (when contact is near the flexure end). At high stiffness values, however, the experimental results are significantly lower than the theoretical results for the flexure alone. This discrepancy is likely associated with higher than expected compliance in VSA components other than the flexure.

Figure 12 is a plot of the free joint range vs. contactor angle for results obtained both experimentally and theoretically. Note that the experimental data closely follows the theoretical curve.

The experimental performance of the Arched Flexure VSA is summarized in Table II for a variety of criteria. Note that the time needed to change stiffness from minimum (zero for small joint motion) to maximum was very short (less than 0.12 s). As noted previously, the Arched Flexure VSA performed as expected except for a significantly lower value for the maximum stiffness. Based on the stiffness of the flexure illustrated in Fig. 10, a stiffness ratio of about 100 or more was expected. The actual stiffness ratio was 55.

Table II Experimental results

Metric	**Results**
Stiffness Ratio	55
Range of Motion	360°
Full Range Variation Time	0.12s

Minimum Stiffness	0.67 Nm/rad
Maximum Stiffness	37 Nm/ad
Overall Size	4.5 in × 2 in × 5 in
Weight	1.44 lb

A. Summary and Conclusions

This paper presented the design and performance of the the Arched Flexure VSA, a structure controlled VSA capable of achieving a large range of stiffness in a small size. A flexure optimized for stiffness range alone was shown to be able to change its stiffness by a factor of more than 1000 in the continuous range and achieve zero stiffness for a small range of joint motion. A smaller range of stiffness (stiffness ratio of about 100) can be attained if a constant relative sensitivity is desired for easier control.

A prototype was fabricated and tested. Experimentation confirmed that a large range of stiffness is achieved (stiffness ratio of 55), but was significantly less than that expected (theoretical stiffness greater than 100). The discrepancy is likely due to the compliance of other load bearing components within the VSA system. A more rugged revision using harmonic drive actuation is planned.

References

1.A. Albu-Schaffer, O. Eiberger, M. Grebenstein, S. Haddadin, C. Ott, T. Wimbock, et al., "Soft robotics: from torque feedback-controlled lightweight robots to intrinsically compliant systems", *IEEE Robotics and Automation Magazine*, vol. 15, no. 3, 2008.

2.G. Pratt and M. Williamson, "Series elastic actuators", *Proceeding of the 1995 IEEE/RSJ International Conference on Intelligent Robots and Systems*, 1995.

3.R. V. Ham, T. G. Sugar, B. Vanderborght, K. W. Hollander and D. Lefeber, "Compliant actuator designs: Review of actuators with passive adjustable compliance/controllable stiffness for robotic applications", *IEEE Robotics and Automation Magazine*, vol. 16, no. 3, 2009.

4.A. Bicchi and G. Tonietti, "Fast and “soft-arm” tactics: Dealing with the safety-performance tradeoff in robot arms design and control", *IEEE Robotics and Automation Magazine*, vol. 11, no. 2, 2004.

5.B. Vanderborght, A. Albu-Schaffer, A. Bicchi, E. Burdet, D. Caldwell, R. Carloni, et al., "Variable impedance actuators: Moving the robots of tomorrow", *Proceeding of the 2012 IEEE/RSJ International Conference on Intelligent Robots and Systems*, 2012.

6."Variable stiffness serial elastic actuator (with large range of stiffness and constant relative sensitivity)".